HHS Public Access

Author manuscript

Methods. Author manuscript; available in PMC 2016 September 27.

Physical characterization and profiling of airway epithelial derived exosomes using light scattering

Mehmet Kesimer[1,*] and **Richa Gupta**[1]

[1] Department of Pathology and Laboratory Medicine, Cystic Fibrosis/Pulmonary Research and Treatment Center, Marsico Lung Institute, University of North Carolina, Chapel Hill, NC 27599-7248

Abstract

Exosomes and other extracellular vesicles have been gaining interest during the last decade due to their emerging role in biology and, disease pathogenesis and their biomarker potential. Almost all published research related to exosomes and other extracellular vesicles include some form of physical characterization. Therefore, these vesicles should be precisely profiled and characterized physically before studying their biological role as intercellular messengers, biomarkers or therapeutic tools. Using a combination of light scattering techniques, including dynamic light scattering (DLS) and multi-angle laser light scattering combined with size exclusion separation (SEC-MALLS), we physically characterized and compared distinct extracellular vesicles derived from the apical secretions of two different cultured airway epithelial cells. The results indicated that epithelial cells release vesicles with distinct physical properties and sizes. Human primary tracheobronchial cell culture (HTBE) derived vesicles have a hydrodynamic radius (*R*h) of approximately 340 nm while their radius of gyration (*R*g) is approximately 200 nm. Electron microscopy analysis, however, revealed that their spherical component is 40-100 nm in size, and they carry filamentous, entangled membrane mucins on their surface that increases their overall radius. The mucin decoration on the surface defines their size and charge as measured using light scattering techniques. Their surface properties mirror the properties of the cells from which they are derived. This may provide a unique tool for researchers to elucidate the unanswered questions in normal airway biology and innate and adaptive defense, including the remodeling of airways during inflammation, tumorigenesis and metastasis.

1. Introduction

Exosomes and other extracellular vesicles have been gaining interest during the last decade due to their emerging role in inter-cellular communication (1, 2), immune modulation (3, 4) and as potential diagnostic in various disease-related conditions (5-7). Exosomes, enclosed

* To whom correspondence should be addressed Mehmet Kesimer, UNC CF Center, 4021 Thurston Bowles, Chapel Hill, NC, 27599-7248, kesimer@med.unc.edu, (919) 843-2577.

The authors declare no conflict of interest

by a phospholipid bilayer, originate in the late endosomal compartment from the inward budding of multi-vesicular bodies (MVBs) (8). Using electron microscopy (EM), these MVBs were observed to bud from the plasma membrane, leading to the secretion of the internal vesicles into the extracellular environment (9, 10). Other extracellular vesicles, however, either fuse from plasma membrane or are shed from polarized epithelia e.g. microvilli (11, 12). Exosomes and other extracellular vesicles are generally isolated using differential centrifugation, column chromatography, filtration or polymeric precipitation and are characterized by a variety of methods including light scattering, particle tracking analysis and EM. Additionally, their cargo is identified via proteomics and miRNA/mRNA analysis. The physical and molecular characteristics of exosomes and other extracellular vesicles depends on the system from which they are derived. They are released into the extracellular space by various cell types including epithelial cells, immune cells, reticulocytes and tumor cells, and are also found in body fluids including saliva (13, 14), urine (15), broncho-alveolar lavage fluid (BALF) (16), airway (17) and cervical mucus (18) plasma (19), and amniotic fluid (20). They carry cargo that contains a distinct set of proteins (21), lipids (22), and RNA (miRNAs, mRNAs) (23). These molecules, which may be a signature of their parent cell, can be horizontally transferred to neighboring cells and thus serve as mediators of intercellular signaling and cellular response.

Secretions from tracheobronchial epithelial cells contain hundreds of innate immune molecules that are released from different types of cells, e.g., secretory and ciliated. These cells also release exosomes and other extracellular vesicles that may be involved in diverse physiological processes in airway biology and in innate (17), and adaptive (24) immune response. Previous studies reported that there is increased vesicle release by bronchial epithelial cells in cystic fibrosis patients (25), and from the lungs of asthmatic patients which induced proliferation and chemotaxis of undifferentiated monocytes (26). In our previous study, we demonstrated that exosomes derived from human HTBE epithelial cells could neutralize human influenza A virus (17) through their sialic acid moieties.

Research on exosomes and other secreted membrane vesicles has expanded in the last decade due to their putative role in therapeutics (27), disease pathogenesis (28) and biomarker discovery (29, 30). These vesicles should be precisely characterized biophysically prior to investigating their role as intercellular messengers, biomarkers or therapeutic tools. In this study, we physically characterized and compared the vesicles isolated from the apical secretions of two different cultured human primary airway epithelial cells (HTBE) and the Calu-3 cell line using three different techniques; Dynamic Light Scattering (DLS), Multi-Angle Laser Light Scattering combined with size exclusion chromatography (SEC-MALLS) and Nanoparticle Tracking Analysis (NTA).

2. Material and Method

2.1 Cell Culture

Two different airway cell culture systems that secrete mucus were used in this study: human tracheobronchial epithelial cells (HTBE) and the airway epithelial Calu-3 cell line. Primary human airway epithelial cells were isolated and cultured as previously described in details (17, 31). Briefly, the cells were plated at a density of 600,000 cells/well on permeable

Transwell-Col (T-Col; 24 mm diameter) support . HTBE cultures were generated by provision of an air–liquid interface for 4–6 week to form well-differentiated, polarized cultures that resemble *in vivo* pseudo-stratified mucociliary epithelium. Airway epithelial Calu-3 cells were derived from pleural effusion associated with a human lung adenocarcinoma. Calu-3 cells were grown on 24-mm Transwell supports (Corning Life Sciences, MA, USA) and maintained at the air–liquid interface for at least three weeks, as previously described (32, 33). Mucus secretions were obtained by performing two sequential 1 mL PBS washes on the apical surface of the cultures. Each wash was collected following a 30 min incubation at 37°C. Culture washings obtained from 6 individual cultures were pooled and centrifuged at 3000 *g* for 10 min to remove the dead cells. Washings were subsequently subjected to differential sedimentation to isolate the exosomes as described below.

2.2 Isolation of Exosomes

Exosomes were isolated using differential centrifugation (17) from HTBE and Calu-3 secretions, which contain complex protein content (34) and are viscous in nature. Briefly, the pooled HTBE and Calu-3 secretions were diluted 1:1 with PBS and were centrifuged at 3000 g for 10 min and 10,000 g for 30 min to eliminate cell debris and other particles. The exosomal vesicles were subsequently pelleted at 65,000 g. The pellet was then washed with PBS and pelleted again at 100,000 g. This washing procedure was repeated to remove any protein or mucin contaminants, which are abundant in the HTBE/Calu-3 secretions. The isolated vesicles were resuspended in PBS and filtered through 0.22-μm filters to eliminate impurities and large-sized micro-particles and spun again at 100,000 g. Finally, the exosome pellets were resuspended in 50 μ L of PBS and stored as 10 μL aliquots at −30° C until further characterization analyses.

2.3 Characterization of Exosomes

2.3.1 Dynamic Light Scattering—The size and zeta potential measurements were conducted using a Zetasizer Nano ZS system (Malvern Instruments, Malvern, U.K.). The dynamic light scattering technique analyzes the velocity distribution of particle movement by measuring the dynamic fluctuations of scattered light intensity at a fixed angle (173°) caused by the Brownian motion of the particle. It assesses the particle perpendicular to the light source at that instant, yielding the particle's hydrodynamic radius (*R*h), or diameter, calculated via the Stokes-Einstein equation (35). DLS also uses a laser that passes through the sample to measure the velocity of the particles in an applied electric field of a known value called the electrophoretic mobility. For DLS measurements, 10 μL exosome aliquots were diluted in 990 μL of PBS (1:100) and then gently mixed to provide a homogeneous solution, and then 1 mL was transferred to a disposable cuvette for size measurements. For Zeta potential measurements, 10 μL exosome aliquot was diluted in 990 μL of water (1:100) and then transferred to a Malvern Clear Zeta Potential cell. Three independent aliquots were analyzed and three measurements were taken for each aliquots.

The data were acquired and analyzed using Dispersion Technology Software (DTS) (V7.01) supplied by the Malvern Zetasizer Nano-ZS.For the particle sizing in solution (DLS), the software provides multiple aspects and interpretations of the data collected for the sample

such as intensity, volume, and number distribution graphs as well as a statistical analysis for each. The mean particle diameter is calculated from the particle distributions measured, and the polydispersity index (PdI) given is a measure of the size ranges present in the solution.

2.3.2 SEC-MALLS analysis—Ten microliter aliquots from the exosome preparations were diluted in 1000 μL PBS. A 500 μ L aliquot was injected and chromatographed on a Sepharose CL-2B column (15×2.5 cm, GE healthcare life sciences) and eluted with 0.2 M NaCl at a flow rate of 500 μ l/min. The column effluent was passed through an inline Dawn DSP laser photometer coupled to a Wyatt/Optilab 903 inferometric refractometer (Wyatt Technologies, Santa Barbara, CA, USA) to measure the molecular weight/radius of gyration and absolute sample concentration. Light scattering measurements were taken continuously at 18 angles between 15° and 151°; the captured data were integrated and analyzed using the Astra software provided with the Dawn photometer.

2.3.3 Nanoparticle Tracking Analysis (NTA)—The detailed characterization of exosomes using NTA is covered as another topic this issue of the Methods. In this study we also used NTA for size and concentration analysis of the isolated exosomes using a NanoSight NS300 instrument equipped with NTA 3.0 analytical software. Each experiment was carried out in triplicate. Each sample was diluted in PBS (1:1000), and mixed before introduction into the sample chamber using a syringe pump with a constant flow rate. Three video recordings, of 60 sec each were initiated. A combination of shutter speed and gain followed by manual focusing enables optimum visualization of a maximum number of vesicles. To accurately track the vesicles they were visualized as single points of light. The samples were advanced between each recording to perform replicate measurements. The NTA post-acquisition settings were optimized and kept constant between the samples, and each video was then analyzed to give the mean, mode, and median vesicle size together with an estimate of the concentration (36).

2.3.4 Electron Microscopy—For electron microscopy (EM) analysis, a one microliter aliquot from the exosome preparation was diluted in 1000 μL of PBS (37). The exosome preparation was fixed with 0.6% glutaraldehyde for 4 minutes and deposited on a thin carbon-coated grid for 5 minutes. The vesicle-coated grids were washed twice with distilled water (1 min each), stained with 2% uranyl acetate; and then viewed with transmission EM (TEM) using a Zeiss EM900 microscope (Carl Zeiss, Oberkochen, Germany). Digital images were taken at 63,000-100,000 magnification.

3. Results and discussion

3.1. Physical profiling of airway extracellular vesicles

Dynamic and static light scattering characterization of vesicles—Hydrodynamic radius (*R*h) of the exosomes was calculated by DLS measurements. The average size in DLS was 342 nm with a polydispersity index (PDI) of 0.426 for HTBE exosomes and 165 nm (PDI = 0.281) for Calu-3 exosomes (Fig.1). The polydispersity index (PDI) was higher for HTBE exosomes indicating a relatively multimodal particle size distribution (figure 1). This may be because the primary human cells that were used in this study are morphologically heterogeneous and thus their exosomes might also be of variable size and shape.

Furthermore, the radius of gyration (*R*g) of the isolated secretory vesicles was measured using static light scattering (MALLS). The angular dependence of scattered light intensity is used to determine the radius of gyration in solution. SEC-MALLS was performed after chromatography on a CL-2B size exclusion column. The exosome preparations were subjected to chromatographic separation on sepharose CL-2B and the average size *R*g and molecular weight (*M*r) distribution were determined across the void peak where the exosomes were eluted on-line MALLS measurements (figure 2). The measurements indicated that the HTBE vesicles are somewhat monodisperse in size (*R*g 200.1 ± 3.0 nm) a with very high average molecular mass (*M*r 7.2×10^7 ±6.973%). As predicted, the *R*g of the HTBE exosomes were smaller than the *R*h measurement obtained from the DLS analysis. The *R*g/*R*h was typically 0.58 which is less than the expected value of a sphere (~0.77) and coils (~0.82). This result might be because of the heterogeneous mixture of the surface mucins radiating from the surface of the vesicles with variable distance (figure 4). MALLS measurements also confirmed that Calu-3 derived exosomes are smaller in size *R*g: 140.2 (±7.8%) nm with an average molecular mass of *M*r 3.875×10^7. The Rg/Rh of the Calu-3 exosomes was 0.84 closer to the expected value of a sphere (~0.77).

NTA measurement is a relatively recently developed technique that determined the size and count of extracellular vesicles (36, 38) and other particles. Here, NTA was performed to determine the size of the vesicles isolated from the two airway cell culture systems. The size distribution of the HTBE exosomes was broader according to this measurement, from 250 nm to 535 nm with an average size 335 nm. The Calu-3 vesicles, however, displayed a monodisperse distribution between 75 nm and 196 nm with an average size of 135 nm. Although closer, the NTA measurements indicated slightly smaller sizes for both the HTBE and Calu-3 vesicles. This finding might be because the DLS measurements are biased toward larger particles while the NTA focuses on all the particles in the field being the measured (39).

Reports from previous studies suggest a range of exosome sizes – between 40 to120 nm depending on the measurement method and the system from which they were isolated (2, 17, 30, 40). Typically vesicles larger than 100-120 nm in size are considered to be exosome-like vesicles or called microparticles (41). Although our DLS measurements indicate relatively larger sized vesicles than previously documented, further EM pictures clarified the difference. Typically, HTBE vesicles/exosomes displayed approximately 40-100 nm cup-shaped spheres with some displaying 100-300 nm entangled filaments emanating from their surface reminiscent of membrane-tethered mucins. Hence, the measurements using light scattering techniques revealed a much greater particle size for the HTBE exosomes (200-400 nm). The Calu-3 exosomes were much smaller and displayed a more typical exosome-like size as observed by EM and measured using light scattering. Some of the Calu-3 derived vesicles also displayed mucin decoration on their surface.

We have previously shown that HTBE exosomes have membrane tethered mucin, predominantly MUC1 (17). Other airway membrane mucins, including MUC4 and MUC16 might also be a part of the surface structure. Electron microscopy analysis confirms this observation by illustrating filamentous and entangled structures of different sizes on the vesicle surfaces. Figure 4 shows how the surface structures affect the size measurements.

This figure compares the light scattering measurements of the HTBE exosomes using the DLS and MALLS techniques. As illustrated the actual vesicular sphere is approximately 100 nm. The MALLS measurements, however, also included the entangled mucin decoration in the estimation. The hydrodynamic radius of this particular vesicle is equal to the radius of a sphere with the same diffusion coefficient as shown with the dotted line at the left panel. The radius of gyration, on the other hand, is calculated from the mean distance of each radiated point (solid lines, R1-R6) from the center of the vesicle at the right panel. DLS measured the *R*h as 342 nm while MALLS measured *R*g as 200 nm. The *R*g/*R*h is typically 0.6 for the vesicles confirming sphere-like structure.

DLS has been extensively used for characterizations of nanoparticles and liposomes and can be employed to study vesicle size and distributions. This method is able to detect and quantify the size increase after vesicle aggregation and fusion. Compared to single-particle imaging techniques, like EM, light scattering obtains information averaged over a fairly large number of particles in a short amount of time. This enables the investigation of a large number of samples in a batch. Furthermore, the amount of sample required is small and reusable. The sample preparation is simple without involving any invasive steps. However, DLS is not without disadvantages. The low refractive index of the vesicles and a bias toward the detection of larger particles when used with heterogeneous solutions can be a drawback when assessing extracellular vesicle.

Zeta potential measurements in liquid reveal the distribution charge density of the molecules and particles – values closer to zero indicate a lower charge. Here we also measured the surface charge of the vesicles derived from airway epithelial cells (table 1). The results indicated that the zeta potential for the HTBE vesicles was on average of −35.6 +/− 1.3 mV, compared the Calu-3 exosomes' potential −31.0 +/− 1.1 mV. Previous studies indicated a zeta potential range from −8 mV to 54 mV for exosomes isolated from different cancer and normal cells (42). The high negative zeta potential of the airway epithelial cells derived vesicles may be due to negatively charged mucins. Sialic acid residues present at the terminal positions of mucins, glycolipids, and other glycoproteins, which have an ionized carboxylate at physiological pH are a major contributor to the net negative charge in biological cells. The amount of sialic acids on an exosome surface may be close to that of the parent cell surface because the glycoproteins of endosomes are supplied from the same organelle and plasma membrane. We previously reported that HTBE derived exosomes-like vesicles are enriched with 2,6 sialic acid on their surface which gives them a unique innate immune function to neutralize the influenza A virus (17).

4- Concluding remarks

Exosomes and other extracellular vesicles related research is increasing because of their potential role in disease pathogenesis and biomarker discovery. Almost all scientific studies related to extracellular vesicles report some type of physical characterization; however, to date, exosome research has been limited by a lack of standardized methods for biophysical profiling. Light scattering techniques such as DLS, MALLS, and, more recently, NTA have been successfully implemented in the field of exosome and other extracellular vesicle research. The light scattering techniques allow specific exosomes and microvesicles in the

range of 40-1000 nm in a liquid suspension to be measured; however, due to the diversity of the vesicles released from different cell types light scattering-based physical measurements should also be confirmed visually using electron microscopy. Here, we provide an example of this suggestion. HTBE vesicles have an approximately 340 nm *R*h according to the DLS measurement and a 200 nm *R*g based upon the MALLS measurements. These values are not suggestive of the previously documented exosomal size, which is typically 40-120 nm. Electron microscopy analysis, however, clearly showed that the spherical parts of the vesicles were approximately 100 nm (figure 4). Because they carry large filamentous entangled structures on their surface, i.e., membrane bound mucins, their actual light scattering based measurement was much larger. Using a combination of techniques, we show here that exosomes derived from cultured airway epithelial cells contain different sizes of membrane-tethered mucins which can alter the physical properties of the structures and affect their measured size, conformation and charges. From a biological and innate mucosal defense perspective, surface mucins carry sites (i.e., sugars) for specific interactions between vesicles and inhaled insults and/or host cells. Thus, their function is critical in normal airway biology and in the pathogenesis of a wide range of diseases, from chronic inflammatory diseases to cancer.

ACKNOWLEDGEMENTS

This study was partly supported by grants from American Lung Association (RG-167538-N) and from the National Institutes of Health (R01HL103940).

References

1. Mittelbrunn M, Sánchez-Madrid F. Intercellular communication: diverse structures for exchange of genetic information. Nature reviews. Molecular cell biology. 2012; 13:328–335. [PubMed: 22510790]
2. Li J, Liu K, Liu Y, Xu Y, Zhang F, Yang H, Liu J, Pan T, Chen J, Wu M, et al. Exosomes mediate the cell-to-cell transmission of IFN-α-induced antiviral activity. Nature immunology. 2013; 14:793–803. [PubMed: 23832071]
3. Chow A, Zhou W, Liu L, Fong MY, Champer J, Van Haute D, Chin AR, Ren X, Gugiu BG, Meng Z, et al. Macrophage immunomodulation by breast cancer-derived exosomes requires Toll-like receptor 2-mediated activation of NF-kappaB. Sci Rep. 2014; 4:5750. [PubMed: 25034888]
4. Williams JL, Gatson NN, Smith KM, Almad A, McTigue DM, Whitacre CC. Serum exosomes in pregnancy-associated immune modulation and neuroprotection during CNS autoimmunity. Clin Immunol. 2013; 149:236–243. [PubMed: 23706172]
5. Duijvesz D, Burnum-Johnson KE, Gritsenko MA, Hoogland AM, Vredenbregt-van den Berg MS, Willemsen R, Luider T, Pasa-Tolic L, Jenster G. Proteomic profiling of exosomes leads to the identification of novel biomarkers for prostate cancer. PLoS One. 2013; 8:e82589. [PubMed: 24391718]
6. Ogata-Kawata H, Izumiya M, Kurioka D, Honma Y, Yamada Y, Furuta K, Gunji T, Ohta H, Okamoto H, Sonoda H, et al. Circulating exosomal microRNAs as biomarkers of colon cancer. PLoS One. 2014; 9:e92921. [PubMed: 24705249]
7. Müller G. Microvesicles/exosomes as potential novel biomarkers of metabolic diseases. Diabetes, metabolic syndrome and obesity : targets and therapy. 2011; 5:247–282.
8. Hurley JH, Odorizzi G. Get on the exosome bus with ALIX. Nat Cell Biol. 2012; 14:654–655. [PubMed: 22743708]
9. Johnstone RM, Adam M, Hammond JR, Orr L, Turbide C. Vesicle formation during reticulocyte maturation. Association of plasma membrane activities with released vesicles (exosomes). J Biol Chem. 1987; 262:9412–9420. [PubMed: 3597417]

10. Théry C, Zitvogel L, Amigorena S. Exosomes: composition, biogenesis and function. Nature reviews. Immunology. 2002; 2:569–579. [PubMed: 12154376]
11. Hara M, Yanagihara T, Hirayama Y, Ogasawara S, Kurosawa H, Sekine S, Kihara I. Podocyte membrane vesicles in urine originate from tip vesiculation of podocyte microvilli. Hum Pathol. 2010; 41:1265–1275. [PubMed: 20447677]
12. McConnell RE, Tyska MJ. Myosin-1a powers the sliding of apical membrane along microvillar actin bundles. J Cell Biol. 2007; 177:671–681. [PubMed: 17502425]
13. Ogawa Y, Taketomi Y, Murakami M, Tsujimoto M, Yanoshita R. Small RNA transcriptomes of two types of exosomes in human whole saliva determined by next generation sequencing. Biol Pharm Bull. 2013; 36:66–75. [PubMed: 23302638]
14. Michael A, Bajracharya SD, Yuen PS, Zhou H, Star RA, Illei GG, Alevizos I. Exosomes from human saliva as a source of microRNA biomarkers. Oral Dis. 2010; 16:34–38. [PubMed: 19627513]
15. Hiemstra TF, Charles PD, Gracia T, Hester SS, Gatto L, Al-Lamki R, Floto RA, Su Y, Skepper JN, Lilley KS, et al. Human urinary exosomes as innate immune effectors. J Am Soc Nephrol. 2014; 25:2017–2027. [PubMed: 24700864]
16. Rodriguez M, Silva J, Lopez-Alfonso A, Lopez-Muniz MB, Pena C, Dominguez G, Garcia JM, Lopez-Gonzalez A, Mendez M, Provencio M, et al. Different exosome cargo from plasma/bronchoalveolar lavage in non-small-cell lung cancer. Genes Chromosomes Cancer. 2014; 53:713–724. [PubMed: 24764226]
17. Kesimer M, Scull M, Brighton B, DeMaria G, Burns K, O'Neal W, Pickles RJ, Sheehan JK. Characterization of exosome-like vesicles released from human tracheobronchial ciliated epithelium: a possible role in innate defense. FASEB journal : official publication of the Federation of American Societies for Experimental Biology. 2009; 23:1858–1868. [PubMed: 19190083]
18. Flori F, Secciani F, Capone A, Paccagnini E, Caruso S, Ricci MG, Focarelli R. Menstrual cycle-related sialidase activity of the female cervical mucus is associated with exosome-like vesicles. Fertil Steril. 2007; 88:1212–1219. [PubMed: 17562335]
19. Muller L, Hong CS, Stolz DB, Watkins SC, Whiteside TL. Isolation of biologically-active exosomes from human plasma. J Immunol Methods. 2014; 411:55–65. [PubMed: 24952243]
20. Asea A, Jean-Pierre C, Kaur P, Rao P, Linhares IM, Skupski D, Witkin SS. Heat shock protein-containing exosomes in mid-trimester amniotic fluids. J Reprod Immunol. 2008; 79:12–17. [PubMed: 18715652]
21. Ji H, Greening DW, Barnes TW, Lim JW, Tauro BJ, Rai A, Xu R, Adda C, Mathivanan S, Zhao W, et al. Proteome profiling of exosomes derived from human primary and metastatic colorectal cancer cells reveal differential expression of key metastatic factors and signal transduction components. Proteomics. 2013; 13:1672–1686. [PubMed: 23585443]
22. Beloribi S, Ristorcelli E, Breuzard G, Silvy F, Bertrand-Michel J, Beraud E, Verine A, Lombardo D. Exosomal lipids impact notch signaling and induce death of human pancreatic tumoral SOJ-6 cells. PLoS One. 2012; 7:e47480. [PubMed: 23094054]
23. Eirin A, Riester SM, Zhu XY, Tang H, Evans JM, O'Brien D, van Wijnen AJ, Lerman LO. MicroRNA and mRNA cargo of extracellular vesicles from porcine adipose tissue-derived mesenchymal stem cells. Gene. 2014; 551:55–64. [PubMed: 25158130]
24. Torregrosa Paredes P, Esser J, Admyre C, Nord M, Rahman QK, Lukic A, Radmark O, Gronneberg R, Grunewald J, Eklund A, et al. Bronchoalveolar lavage fluid exosomes contribute to cytokine and leukotriene production in allergic asthma. Allergy. 2012; 67:911–919. [PubMed: 22620679]
25. Porro C, Lepore S, Trotta T, Castellani S, Ratclif L, Battaglino A, Di Gioia S, Martínez MC, Conese M, Maffione AB. Isolation and characterization of microparticles in sputum from cystic fibrosis patients. Respiratory research. 2009; 11:94. [PubMed: 20618958]
26. Kulshreshtha A, Ahmad T, Agrawal A, Ghosh B. Proinflammatory role of epithelial cell-derived exosomes in allergic airway inflammation. The Journal of allergy and clinical immunology. 2013; 131:1194. [PubMed: 23414598]

27. Pitt JM, Charrier M, Viaud S, André F, Besse B, Chaput N, Zitvogel L. Dendritic cell-derived exosomes as immunotherapies in the fight against cancer. Journal of immunology (Baltimore, Md. : 1950). 2014; 193:1006–1011.

28. Fiandaca MS, Kapogiannis D, Mapstone M, Boxer A, Eitan E, Schwartz JB, Abner EL, Petersen RC, Federoff HJ, Miller BL, et al. Identification of preclinical Alzheimer's disease by a profile of pathogenic proteins in neurally derived blood exosomes: A case-control study. Alzheimers Dement. 2014

29. Jayaram S, Gupta MK, Polisetty RV, Cho WC, Sirdeshmukh R. Towards developing biomarkers for glioblastoma multiforme: a proteomics view. Expert review of proteomics. 2014; 11:621–639. [PubMed: 25115191]

30. Zheng X, Chen F, Zhang J, Zhang Q, Lin J. Exosome analysis: a promising biomarker system with special attention to saliva. J Membr Biol. 2014; 247:1129–1136. [PubMed: 25135166]

31. Fulcher ML, Gabriel S, Burns KA, Yankaskas JR, Randell SH. Well-differentiated human airway epithelial cell cultures. Methods Mol Med. 2005; 107:183–206. [PubMed: 15492373]

32. Kreda SM, Okada SF, van Heusden CA, O'Neal W, Gabriel S, Abdullah L, Davis CW, Boucher RC, Lazarowski ER. Coordinated release of nucleotides and mucin from human airway epithelial Calu-3 cells. J Physiol. 2007; 584:245–259. [PubMed: 17656429]

33. Cao R, Wang TT, DeMaria G, Sheehan JK, Kesimer M. Mapping the protein domain structures of the respiratory mucins: a mucin proteome coverage study. J Proteome Res. 2012; 11:4013–4023. [PubMed: 22663354]

34. Kesimer M, Kirkham S, Pickles RJ, Henderson AG, Alexis NE, Demaria G, Knight D, Thornton DJ, Sheehan JK. Tracheobronchial air-liquid interface cell culture: a model for innate mucosal defense of the upper airways? American journal of physiology. Lung cellular and molecular physiology. 2008:296.

35. Edward JT. Molecular volumes and the Stokes-Einstein equation. Journal of Chemical Education. 1970; 47:261.

36. Dragovic RA, Gardiner C, Brooks AS, Tannetta DS, Ferguson DJ, Hole P, Carr B, Redman CW, Harris AL, Dobson PJ, et al. Sizing and phenotyping of cellular vesicles using Nanoparticle Tracking Analysis. Nanomedicine. 2011; 7:780–788. [PubMed: 21601655]

37. Thery C, Amigorena S, Raposo G, Clayton A. Isolation and characterization of exosomes from cell culture supernatants and biological fluids. Curr Protoc Cell Biol Chapter 3:Unit 3. 2006:22.

38. Momen-Heravi F, Balaj L, Alian S, Tigges J, Toxavidis V, Ericsson M, Distel RJ, Ivanov AR, Skog J, Kuo WP. Alternative methods for characterization of extracellular vesicles. Front Physiol. 2012; 3:354. [PubMed: 22973237]

39. Gercel-Taylor C, Atay S, Tullis RH, Kesimer M, Taylor DD. Nanoparticle analysis of circulating cell-derived vesicles in ovarian cancer patients. Anal Biochem. 2012; 428:44–53. [PubMed: 22691960]

40. Schneider A, Simons M. Exosomes: vesicular carriers for intercellular communication in neurodegenerative disorders. Cell Tissue Res. 2013; 352:33–47. [PubMed: 22610588]

41. Geddings JE, Mackman N. Tumor-derived tissue factor-positive microparticles and venous thrombosis in cancer patients. Blood. 2013; 122:1873–1880. [PubMed: 23798713]

42. Sokolova V, Ludwig AK, Hornung S, Rotan O, Horn PA, Epple M, Giebel B. Characterisation of exosomes derived from human cells by nanoparticle tracking analysis and scanning electron microscopy. Colloids Surf B Biointerfaces. 2011; 87:146–150. [PubMed: 21640565]

- Exosomes should be characterized physically before studying their biological role
- Airway epithelial cells release vesicles with distinct physical properties and sizes
- HTBE exosomes have a hydrodynamic radius of 340 nm and radius of gyration is 200 nm
- EM, however, shows their spherical component is 40-100 nm in size
- They carry entangled membrane mucins on their surface that defines their radius and function

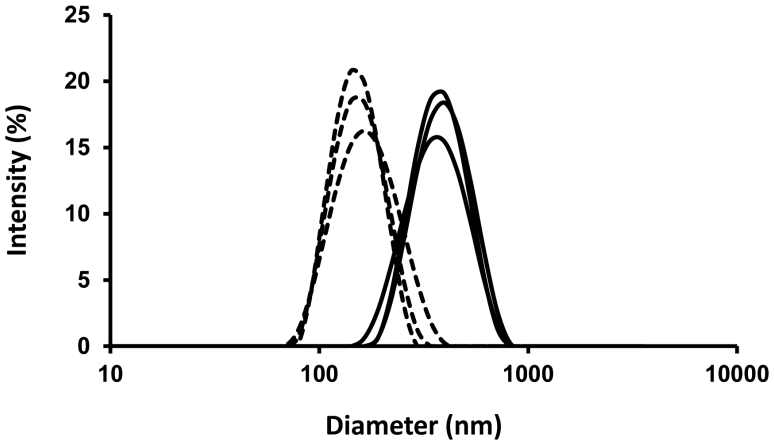

Figure 1. Size distribution of HTBE and Calu-3 vesicles

Percentage intensity size distribution of exosomes from Calu-3 (dashed lines) and HTBE (solid lines) cells by dynamic light scattering. Ten microliter of an exosome aliquot was diluted in 990 μl of PBS and transferred to a disposable cuvette. Three DLS data sets were acquired and the mean particle diameter is calculated using the DTS (V7.01) software. The average size of Calu-3 exosomes is 165 nm and of HTBE exosomes is 342 nm.

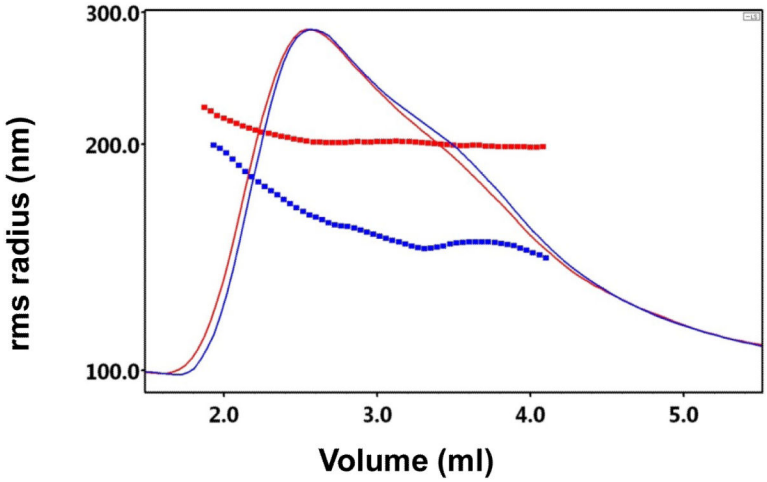

Figure 2. SEC-MALLS analysis of HTBE and Calu-3 vesicles

Isolated vesicles were separated by chromatography on a Sepharose CL-2B column at a flow rate of 0.5 mL/min in 0.2 M NaCl and the effluent was monitored for 18 light scattering angle to determine size and refractive index to determine samples concentration (solid lines). Radius of gyration measurements (*R*g, dotted lines) were plotted across the (V_o) exosome peak (solid lines). The HTBE exosomes displayed an average *R*g of 202 nm (Red), while the Calu-3 exosomes displayed an average *R*g of 145 nm (blue) across the distribution.

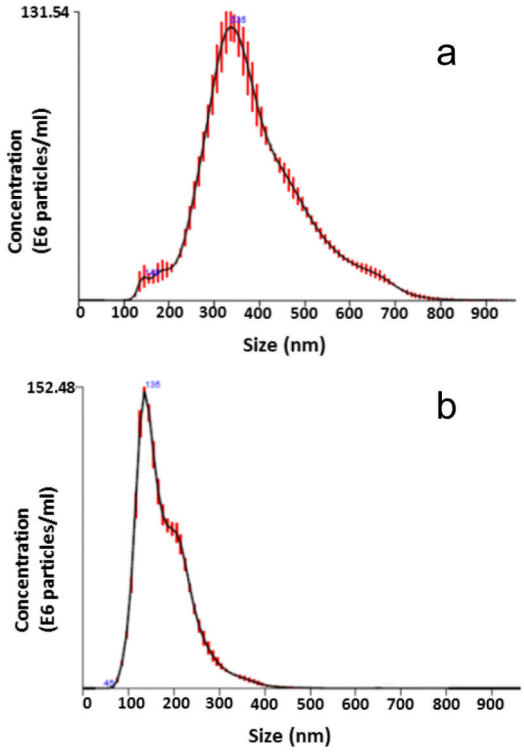

Figure 3. NTA of HTBE and Calu-3 vesicles

Size distribution curve of extracellular vesicles from a) HTBE cells, and b) Calu-3 cells, using NanoSight. Each experiment was carried out in triplicate. The samples were diluted in PBS (1:1000) and mixed before introduction into the sample chamber using a syringe pump with a constant flow rate. Three video recordings, of 60 sec each were initiated. A combination of shutter speed and gain followed by manual focusing enables optimum visualization of a maximum number of vesicles. NTA post-acquisition settings were optimized and kept constant between the samples, and each video was then analyzed to give the mean, mode, and median vesicle size together with an estimate of the concentration.

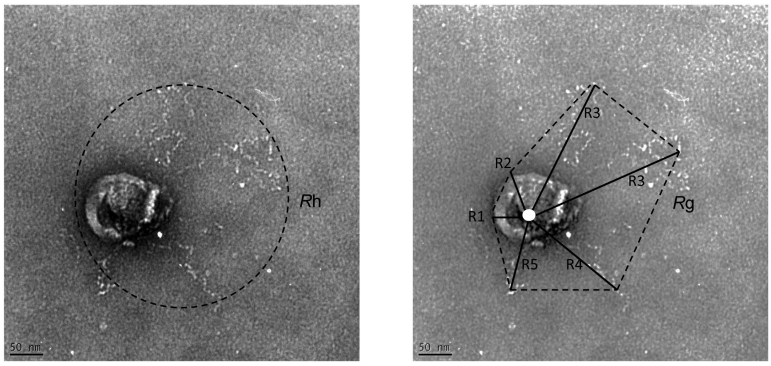

Figure 4. Illustration of two light scattering measurements of HTBE exosomes (with mucin decoration on the surface) using DLS (left) and MALLS (right) techniques

As can be estimated from the picture the actual vesicular sphere is approximately 100 nm. The light scattering measurements, however, also include the mucin decoration in the estimate. **Left:** The hydrodynamic radius (*R*h) of this particular vesicle will be equal to the radius of a sphere with the same diffusion coefficient as shown with the dotted line. **Right:** The radius of gyration (mean square root, MSR) is calculated using the mean distance of each radiated point (solid lines, R1-R6) from the center of the vesicle. DLS measures the *R*h to be 340 nm, while MALLS measured the *R*h to be 200 nm. The *R*g/*R*h is typically 0.6 for these vesicles.

Table 1

Zeta potential measurement of HTBE and Calu-3 vesicles using DLS.

Sample	1	2	3	Z-average
HBE vesicles	−35.3	−36.7	−34.8	−35.6
Calu-3 vesicles	−29.3	−32.7	−31.1	−31.0